

Teacher-Guided Policy Optimization for LLM Distillation

Xinyu Liu¹ Kechen Jiao² Chunyang Xiao Runsong Zhao¹ Junhao Ruan¹ Bei Li³ Jiahao Liu³
 Qifan Wang⁴ Xin Chen³ Jingang Wang³ Tong Xiao^{1,5} JingBo Zhu^{1,5}

Abstract

The convergence of reinforcement learning and imitation learning has positioned Reverse KL (RKL) as a promising paradigm for on-policy LLM distillation, aiming to unify exploration with teacher supervision. However, we identify a critical limitation: when the student and teacher distributions diverge significantly, standard RKL often fails to yield meaningful improvement due to uninformative negative feedback. To address this inefficiency, we propose Teacher-Guided Policy Optimization (TGPO), an on-policy algorithm that incorporates dense directional guidance by leveraging teacher predictions conditioned on the student’s rollout. Because TGPO remains on-policy, the algorithm integrates seamlessly with existing RLVR frameworks without requiring additional data annotation. Experiments on complex reasoning benchmarks demonstrate that TGPO significantly outperforms standard baselines and is robust to different teachers.

1. Introduction

As Large Language Models (LLMs) become ubiquitous tools in daily life, deploying them in latency-sensitive or cost-constrained environments remains a challenge. To address this, LLM distillation is often employed to transfer knowledge from a large-scale, capable teacher to a smaller student model (Hinton et al., 2015), enabling efficient inference without sacrificing reasoning capability.

Traditionally, LLM distillation operates off-policy, where the student mimics teacher trajectories via Supervised Fine-Tuning (SFT). While efficient, this paradigm is fundamentally hindered by distribution shift (exposure bias): the discrepancy between teacher-forced training and autonomous inference leads to cascading errors upon deviation (Chu

¹School of Computer Science and Engineering, Northeastern University, China ²Tsinghua University ³Meituan ⁴Meta AI ⁵NiuTrans Research, Shenyang, China. Correspondence to: Xinyu Liu <lxy1051493182@gmail.com>.

Preprint.

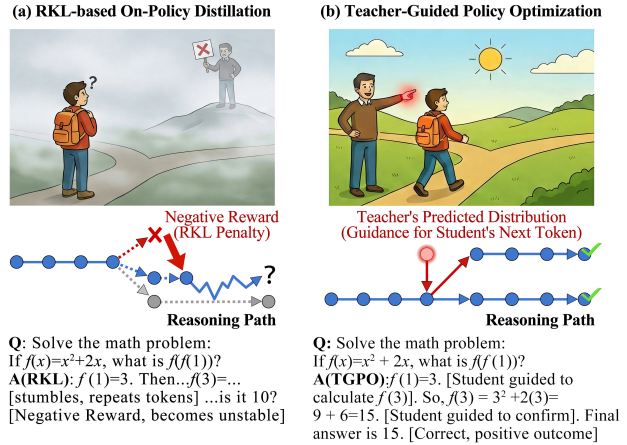


Figure 1. **RKL vs. TGPO.** (a) RKL relies on scalar rewards to penalize deviation. When the policy gap is significant, these penalties fail to provide directional information. (b) TGPO utilizes the teacher’s predicted distribution as **guidance**, explicitly informing the student *what* to generate next rather than *what not* to generate.

et al., 2025), resulting in a rigid model with limited exploration capabilities (Chen et al., 2025). Conversely, recent advances in post-training prioritize on-policy exploration, exemplified by Reinforcement Learning (RL) with Verifiable Rewards (RLVR) or outcome-based supervision (Guo et al., 2025; Jaech et al., 2024; Team et al., 2025). However, these pure RL approaches require navigating vast combinatorial search spaces, making them computationally prohibitive for smaller models or early training stages where the model lacks basic reasoning proficiencies.

To bridge the gap between effective teacher supervision and on-policy exploration, the community has recently converged on on-policy distillation (Agarwal et al., 2024; Lu & Lab, 2025; Xu et al., 2025), typically formulated as minimizing the Reverse Kullback-Leibler (RKL) divergence ($D_{\text{KL}}(\pi_{\text{student}}||\pi_{\text{teacher}})$). Unlike SFT, the RKL objective is estimated using trajectories sampled from the student, ensuring structural alignment with RL algorithms. By allowing the student to explore its own support while receiving feedback via likelihood ratios from the teacher, RKL theoretically offers a unified framework that combines the exploration benefits of RLVR with teacher supervision.

Despite its theoretical elegance, we identify a critical failure

mode in standard RKL when applied to complex reasoning. When a significant distributional gap exists between the student and teacher, RKL suffers from severe instability and often fails to converge, which severely limits its practical utility. In Section 2, we mathematically analyze this failure mode, revealing that RKL restricts the teacher to the role of a post-hoc discriminator, merely evaluating the quality of student samples. Crucially, the teacher fails to provide constructive guidance (i.e., indicating the optimal token), leaving the student to explore blindly. This issue is amplified under significant distributional shift: the teacher assigns negligible probabilities to a significant number of student-generated tokens, yielding uninformative gradients that constrain exploration rather than steering the student back to the optimal distribution.

To address these limitations, we propose Teacher-Guided Policy Optimization (TGPO), a novel on-policy distillation framework designed to provide informative, directional updates even when distributions differ. As illustrated in Figure 1, unlike RKL, which evaluates the teacher’s likelihood of the student’s actions, TGPO queries the teacher for the optimal action given the student’s generated context. By maximizing the likelihood of the teacher’s predicted tokens on the student’s rollout, TGPO leverages the exploration benefits of on-policy sampling while retaining the constructive supervision of supervised learning. Crucially, this mechanism enriches traditional on-policy RL with fine-grained, token-level supervision, bridging the gap between sparse outcome rewards and dense teacher guidance. In summary, by investigating how to incorporate teacher’s knowledge for LLM distillation inside an *on-policy* RL framework, we have made the following contributions:

- We provide an analysis of the standard RKL framework for LLM distillation. We show that RKL does not effectively leverage the teacher’s guidance, which restricts its applicability by causing training instability when significant distributional gaps exist between the teacher and student. We validate this instability in Section 2.
- Guided by the RKL analysis, we propose a novel on-policy distillation framework in Section 3. Our approach is based on the teacher’s token predictions, functioning similarly to SFT but integrated into the on-policy generation process. We also address critical design choices, such as whether to incorporate the teacher signal into the reward or into the loss function as regularization.
- Experimental results demonstrate that our method is effective for on-policy distillation. Not only it is able to mitigate existing RKL distillation problem and learn from far-away distributions, but also it is competitive with mix-policy approaches.

2. RKL Limitations in LLM Distillation

In this section, we first (Subsection 2.1) mathematically formulate the LLM distillation problem using RKL and show how it promisingly integrates with reinforcement learning (RL) formulations. In Subsection 2.2, we dive deeper into the RKL formulation and discuss its inefficiency to integrate teacher’s knowledge as well as the potential instability issues which we empirically validate in the end of this section.

2.1. RKL-Based On-Policy Distillation

In the context of LLMs, consider a dataset $\mathcal{D} = \{x\}$ of prompts. Let y denote the corresponding response generated by a policy. We aim to train a student policy $\pi_\theta(y|x)$ to approximate a fixed, superior teacher policy $\pi_T(y|x)$. Recently, on-policy distillation methods (Gu et al., 2023; Team et al., 2024; Agarwal et al., 2024) have gained popularity, where the student learns to approximate the teacher’s distribution by minimizing the Reverse KL (RKL) divergence:

$$\begin{aligned} \mathcal{J}_{\text{RKL}}(\theta) &= \mathbb{E}_{x \sim \mathcal{D}} D_{\text{KL}}(\pi_\theta || \pi_T) \\ &= \mathbb{E}_{x \sim \mathcal{D}, y \sim \pi_\theta(\cdot|x)} \left[\log \frac{\pi_\theta(y|x)}{\pi_T(y|x)} \right]. \end{aligned} \quad (1)$$

Crucially, as explicitly shown in Eq. 1, the RKL objective involves an expectation over the *student’s* own generation distribution ($y \sim \pi_\theta$). This contrasts with Forward KL or SFT, which rely on samples from the teacher’s distribution. Since RL algorithms fundamentally rely on such on-policy sampling to learn from rewards, this structural alignment facilitates the integration of RKL into RL frameworks.

By defining $r(y)$ as the reward function for a sampled sequence y , we can explicitly compare the objectives:

$$\mathcal{J}_{\text{RL}}(\theta) = \mathbb{E}_{x \sim \mathcal{D}, y \sim \pi_\theta(\cdot|x)} [r(y)] \quad (2)$$

Comparing Eq. 1 and Eq. 2, it becomes evident that minimizing \mathcal{J}_{RKL} is mathematically equivalent to maximizing \mathcal{J}_{RL} with intrinsic reward $r(y) = -\log \frac{\pi_\theta(y|x)}{\pi_T(y|x)}$.

Given the above observations, we can integrate the RKL and RL objectives via two primary mechanisms. The first approach formulates the log-ratio as an intrinsic reward, utilizing standard RL algorithms to maximize the augmented reward $r(y) - \log \frac{\pi_\theta(y|x)}{\pi_T(y|x)}$. Alternatively, one can treat \mathcal{J}_{RKL} as a differentiable regularization term, optimizing it via gradient descent on samples drawn from the student π_θ , while \mathcal{J}_{RL} is handled by the RL optimizer.¹

¹Note that these formulations imply different gradient dynamics: the reward-based approach treats the log-ratio as a scalar weight, whereas the regularization approach directly backpropagates through the student’s log-probabilities.

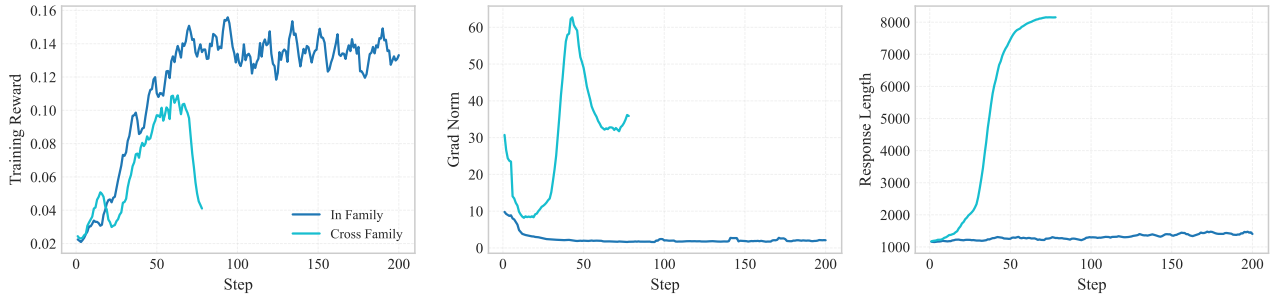


Figure 2. Comparison of RKL distillation dynamics. We distill a Qwen2.5-Math-1.5B student using either an In-Family teacher (Qwen2.5-Math-7B) or a Cross-Family teacher (Qwen3-30B-A3B). While the In-Family setting converges stably, the Cross-Family setting exhibits catastrophic instability, characterized by sharp training score degradation (**Left**), gradient norm spikes (**Middle**), and unbounded response length growth (**Right**).

2.2. The Limitations of RKL-based Methods

While theoretically attractive for its simplicity, we argue that the RKL objective is fundamentally flawed when operating in low-reward regimes which we detail below. In this section, we focus our analysis on the framework where RKL serves as an intrinsic reward, following recent works (Xu et al., 2025; Lu & Lab, 2025).

Since trajectories y are sampled directly from the student policy $\pi_\theta(\cdot|x)$, they inherently cluster in regions where the student assigns high probability mass. Let $\rho(y) = \frac{\pi_\theta(y|x)}{\pi_T(y|x)}$ denote the density ratio. Noting that the intrinsic reward $-\log \rho(y)$ decreases monotonically as $\rho(y)$ increases, we categorize the optimization landscape into two scenarios²:

- $\rho(y) \approx 1$ (**Consensus**): The student’s generation lies within the teacher’s high-probability support. The density ratio is near unity, yielding a neutral intrinsic reward ($-\log \rho(y) \approx 0$).
- $\rho(y) \gg 1$ (**Rejection**): The student assigns high probability to samples the teacher rejects. This results in a large density ratio and a severe penalty ($-\log \rho(y) \ll 0$).

In the Consensus regime, successful rollouts are naturally reinforced by the RL algorithm. However, in the Rejection regime, the teacher functions merely as a punitive critic, providing a negative scalar signal without offering constructive guidance on the optimal token (i.e., the correct target). Consequently, the student is forced to navigate the vast action space via inefficient trial-and-error, often leading to optimization stagnation. As illustrated in Figure 1(a), the lack of directional correction makes escaping the low-reward region computationally intractable.

Beyond the lack of directional guidance, we identify a critical asymmetry in reward scaling. While the probability ratio

²Crucially, as we sample from π_θ , we rarely observe instances where $\pi_\theta(y|x) \ll \pi_T(y|x)$ (i.e., $\rho(y) \ll 1$). This implies the student rarely receives high positive rewards for “discovering” teacher modes it does not currently cover, a fundamental limitation of on-policy sampling.

$\rho(y)$ is theoretically unbounded from above (leading to infinite penalties when $\pi_T \rightarrow 0$), it is effectively lower-bounded by the student’s own probability $\pi_\theta(y|x)$ (since $\pi_T \leq 1$). Because trajectories are sampled from the student where π_θ is relatively high, the ratio rarely drops significantly below 1. Consequently, the positive reward is structurally capped, whereas the negative penalty can diverge toward infinity. This extreme imbalance means that a single “bad” sample can generate a gradient magnitude that disproportionately dominates the accumulated positive signals from “good” samples, destabilizing the optimization. We provide a formal derivation of these gradient dynamics and their impact on stability in Appendix A.

Finally, we remark that treating RKL as a differentiable regularizer does not resolve the fundamental issue of blind exploration. Since the objective relies on student sampling, the teacher remains a passive evaluator, unable to steer the student toward optimal modes it has not yet visited.

2.3. Empirical Validation

Based on our analysis, we conjecture that training stability and performance will degrade significantly when the student frequently generates tokens yielding high density ratios ($\rho(y) \gg 1$). Unfortunately, this scenario is ubiquitous in practical LLM distillation where inherent distributional shifts exist between the student and teacher, particularly when they differ in model architecture or capacity. While prior works (Gu et al., 2023; Xu et al., 2025) show that it is also possible to bring student distribution and teacher distribution quite close to mitigate the problem, we argue that such approaches greatly limit RKL practical applicability.

To validate our analysis, we examine the behavior of RKL-based distillation on a mathematical reasoning task. We isolate the impact of RKL by integrating it as the sole reward signal within an RL framework. We use a Qwen2.5-Math-1.5B student under two distinct configurations de-

signed to represent varying degrees of distributional shift³:

- **In-Family Distillation:** We employ Qwen2.5-Math-7B as the teacher. Since both models share the same architecture family and training data distribution, the distribution mismatch is minimal.
- **Cross-Family Distillation:** We utilize Qwen3-30B-A3B as the teacher⁴. This larger, generalist model possesses a different latent space and reasoning patterns, amplifying the support divergence.

Result. The training dynamics are visualized in Figure 2. Note that while the policy is optimized solely via the intrinsic RKL reward, we monitor the average task reward on the MATH training dataset to gauge semantic correctness. The results reveal a striking dichotomy between the two settings. In the In-Family scenario, the student converges steadily, effectively distilling knowledge from the teacher and achieving consistent gains in task accuracy. This confirms that RKL functions well when π_θ and π_T are initially aligned. Conversely, the Cross-Family setting is plagued by severe instability. Consistent with our analysis of the “Rejection” regime, we observe: (1) Performance Collapse, where the model fails to improve monotonically, with task rewards oscillating or degrading; (2) Exploding Gradients, characterized by consistently high gradient norms that indicate unbounded penalties are destabilizing the optimizer; and (3) Distributional Divergence, where the student significantly deviates from its original distribution (e.g., pathological length drift) after only ~ 100 steps.

3. Teacher-Guided Policy Optimization

To address the limitations identified in Section 2, in this section, we propose a novel LLM distillation algorithm **Teacher-Guided Policy Optimization (TGPO)**. Similar to RKL, our algorithm remains on-policy and is thus easy to integrate into RL frameworks. However, unlike RKL-based approaches that utilize the teacher primarily to impose distributional constraints or modulate rewards, TGPO fundamentally transforms the teacher’s role from a *post-hoc discriminator* (judging the output) to an *ante-hoc guide* (suggesting the next step), enabling the student to effectively leverage the supervision signals from teacher-derived targets while retaining the benefits of reinforcement learning.

3.1. Step-wise Guidance on Student Trajectories

Consistent with the motivation of RKL, our approach adheres to an on-policy framework, relying solely on rollouts

³Detailed experimental settings and hyperparameters are provided in Appendix B.1.

⁴We select the reasoning-intensive “thinking” MoE model as a proxy for a high-capability generalist model, representing a distinct distribution from the specialized math student.

from the student policy π_θ . Specifically, let $y \sim \pi_\theta(\cdot|x)$ denote a trajectory generated by the student, where at each step t , the token y_t is sampled based on the prefix $y_{<t}$.

To address the lack of directional feedback in RKL, we incorporate a *guidance* term derived from the teacher’s local optimality. Figure 3 illustrates this process, where for every state $y_{<t}$ visited by the student, we compute the teacher’s optimal next token $y_t^T = \operatorname{argmax}_{v \in \mathcal{V}} \pi_T(v|x, y_{<t})$. We then formulate the guidance objective as maximizing the likelihood of this target token:

$$\mathcal{J}_{\text{Guidance}}(\theta) = \mathbb{E}_{x \sim \mathcal{D}, y \sim \pi_\theta} \left[-\frac{1}{|y|} \sum_{t=1}^{|y|} \log \pi_\theta(y_t^T | x, y_{<t}) \right]. \quad (3)$$

This formulation stands in sharp contrast to the RKL objective. While RKL provides only a scalar *judgment* (reward) on the student’s choice, our objective provides *dense supervision*, directly suggesting the optimal token to guide the student toward high-likelihood regions that it might otherwise fail to discover via its own exploration.

Mechanistically, the log-likelihood term resembles the teacher-forcing objective used in SFT. However, a critical distinction lies in the trajectory distribution: our samples y are drawn from the student policy (π_θ) rather than the static ground truth. This ensures that the teacher’s guidance is dynamic; it corrects the student based on the student’s *actual* current state, thereby mitigating the distribution shift and exposure bias issues associated with offline SFT.

3.2. Integrating Guidance into GRPO

Leveraging the on-policy nature of our guidance framework, we seamlessly integrate it into Group Relative Policy Optimization (GRPO) (Shao et al., 2024). We select GRPO for its proven computational efficiency and stability, particularly in reasoning tasks where it eliminates the need for a separate value function.

Formally, given a query $x \sim \mathcal{D}$, the policy π_θ generates a group of G outputs $\{y_i\}_{i=1}^G$. Following the design of GRPO and recent advancements (Yu et al., 2025; He et al., 2025; Liu et al.), we omit the explicit KL divergence penalty relative to the reference model and operate directly on token-level gradients. The optimization objective is defined as:

$$\mathcal{J}_{\text{GRPO}}(\theta) = \mathbb{E}_{x \sim \mathcal{D}, y \sim \pi_\theta} \left[\frac{1}{Z} \sum_{i=1}^G \sum_{t=1}^{|y_i|} \rho_{i,t}(\theta) A_i \right], \quad (4)$$

where $Z = \sum_i |y_i|$ serves as the normalization factor based on the total token count. Here, $\rho_{i,t}(\theta) = \frac{\pi_\theta(y_{i,t}|x, y_{i,<t})}{\pi_{\theta_{\text{old}}}(y_{i,t}|x, y_{i,<t})}$ denotes the importance sampling ratio. The term $A_i = \frac{r_i - \mu}{\sigma}$ represents the advantage, where r_i is the reward associated

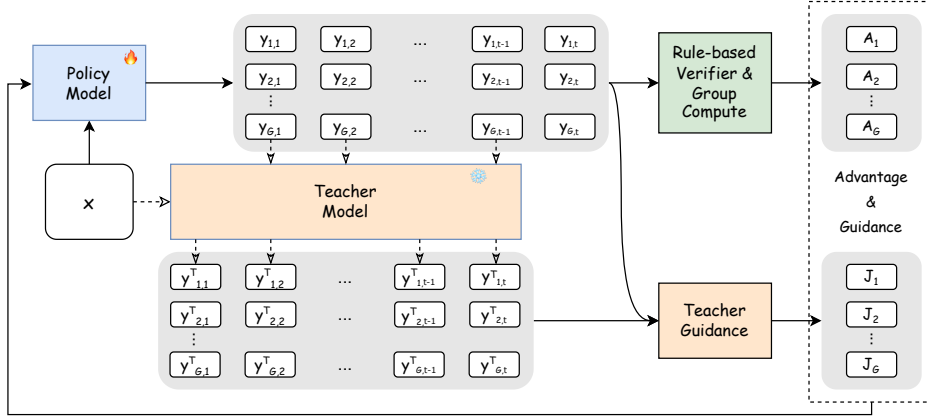


Figure 3. Overview of the TGPO. The Policy Model generates a group of rollouts $\{y_i\}_{i=1}^G$ conditioned on input x . At each step, the Teacher Model provides dynamic token-level guidance by predicting the optimal target token y^T based on the student’s current prefix. This dense guidance signal (J) complements the outcome-based advantage (A) derived from the Rule-based Verifier to update the policy.

with sequence y_i (e.g., rule-based scores), standardized using the group’s mean μ and standard deviation σ .

Similar to the integration strategies discussed in Section 2.1, embedding the step-wise guidance $\mathcal{J}_{\text{Guidance}}$ (defined in Sec. 3.1) into the GRPO framework presents a critical design choice regarding the nature of the teacher’s influence. We identify two primary paradigms for combining such guidance with RL objectives:

Reward Shaping. This approach incorporates the teacher’s feedback directly into the advantage estimation. Specifically, we augment the group relative advantage A_i with the guidance term. The guidance term hereby rewards student’s token $y_{i,t}$ when it obtains approval from the teacher’s target $y_{i,t}^T$. The integrated objective can be formulated as:

$$\mathcal{J}_{\text{TGPO}}^R(\theta) = \mathbb{E}_{x \sim \mathcal{D}, y \sim \pi_\theta} \left[\frac{1}{Z} \sum_{i=1}^G \sum_{t=1}^{|y_i|} \rho_{i,t}(\theta) \hat{A}_{i,t} \right], \quad (5)$$

where the augmented advantage is defined as $\hat{A}_{i,t} = A_i + \lambda \cdot \text{sg}[\log \pi_\theta(y_{i,t}^T | x, y_{i,<t})]$. Here, λ controls the magnitude of the shaping term, and $\text{sg}[\cdot]$ denotes the stop-gradient operator. Crucially, in this formulation, the guidance signal functions solely as a scalar reward value detached from the computational graph, meaning it does not provide a direct differentiable path for updating the policy parameters.

Differentiable Regularization. Alternatively, this approach treats the teacher’s target y_i^T as a direct supervision label, akin to SFT, but calculated dynamically on student trajectories. The joint optimization objective is:

$$\mathcal{J}_{\text{TGPO}}^D(\theta) = \mathcal{J}_{\text{GRPO}}(\theta) + w \mathcal{J}_{\text{Guidance}}(\theta), \quad (6)$$

where w is a weighting hyperparameter. In contrast to reward shaping, this formulation injects a dense gradient signal by directly differentiating through the guidance term,

thereby explicitly shaping the policy parameters to maximize the likelihood of the teacher’s target.

Although the two formulations may appear superficially similar—differing primarily in whether the guidance term is placed inside or outside the expectation—we emphasize that they are mathematically non-equivalent. The distinction lies in the gradient mechanics: Reward Shaping relies on the score function estimator (REINFORCE) where the guidance acts as a weight for the student’s sampled path, whereas Differentiable Regularization provides a direct path-wise derivative toward the teacher’s target token. We provide the full derivation of these gradients in Appendix A and empirically analyze their impact in Section 4. Intuitively, Reward Shaping relies on the student’s exploration to discover high-reward regions, while Differentiable Regularization actively pulls the student toward the teacher’s preference via imitation. While we empirically investigate both strategies, TGPO adopts the Differentiable Regularization formulation to leverage these dense gradient signals for effective reasoning bootstrapping.

Although strong initial guidance effectively bootstraps reasoning, rigid supervision later in training may restrict the student’s exploration capabilities. Therefore, to balance imitation and exploration, we employ a linearly decaying schedule for the guidance weight w : $w_t = \max(w_{\text{init}} - \delta \cdot t, 0)$, where w_{init} denotes the initial weight strength, t represents the current training step, and δ is the decay rate per step. This schedule facilitates robust initial alignment followed by a smooth transition toward pure reward-driven optimization, ensuring the student eventually learns to rely on its own reasoning process. We refer to this specific configuration as **TGPO-annealing**.

Model	In-Distribution Performance						Out-of-Distribution Performance			
	AIME 24/25	AMC	MATH-500	Minerva	Olympiad	Avg.	ARC-c	GPQA*	MMLU-Pro	Avg.
Original Models										
Qwen2.5-Math-7B	11.5/4.9	31.3	43.6	7.4	15.6	19.0	18.2	11.1	16.9	15.4
Qwen3	59.5/49.8	85.3	96.0	52.9	68.0	68.6	94.1	65.2	80.0	79.8
Qwen3-8192	25.1/17.4	52.2	86.2	47.4	47.7	46.0	93.8	49.0	76.5	73.1
Off-Policy and Mixed-Policy Methods										
SFT	12.9/15.1	45.3	80.4	42.3	41.0	39.5	73.1	20.2	44.9	46.1
LUFFY	19.6/14.9	57.6	83.6	38.6	51.9	<u>44.4</u>	80.1	38.9	50.1	<u>56.4</u>
On-Policy Methods										
SimpleRL-Zero	27.0/6.8	54.9	76.0	25.0	34.7	37.4	30.2	23.2	34.5	29.3
PRIME-Zero	17.0/12.8	54.0	81.4	39.0	40.3	40.7	73.3	18.2	32.7	41.4
Oat-Zero	33.4/11.9	61.2	78.0	34.6	43.4	43.7	70.1	23.7	41.7	45.2
GRPO++	19.5/15.8	58.3	82.2	37.5	47.3	43.4	77.4	32.3	46.9	52.1
KDRL	17.2/14.4	55.8	83.6	36.0	43.4	41.7	78.4	35.4	46.9	53.6
OP Distill	5.7/4.5	29.9	64.0	23.2	27.1	25.7	26.1	6.1	23.0	18.4
TGPO_R	21.0/ <u>17.3</u>	58.4	<u>84.2</u>	33.1	47.3	43.6	80.1	33.3	48.1	53.8
TGPO	20.1/16.0	<u>58.6</u>	83.6	37.9	48.1	44.1	<u>81.2</u>	<u>37.9</u>	48.9	56.0
TGPO-annealing	<u>21.1/17.9</u>	60.2	84.4	<u>40.4</u>	<u>49.8</u>	45.6	82.8	37.4	50.1	56.8

Table 1. In-distribution and out-of-distribution performance based on Qwen2.5-Math-7B. We primarily benchmark against on-policy baselines, while also including off-policy and mixed-policy methods for comparison. The teacher model employed is Qwen3-30B-A3B (Qwen3); we additionally report its performance with a maximum generation length of 8192 tokens (Qwen3-8192). All models are evaluated under a unified setting. Bold indicates the best result, and underline indicates the second best (excluding the teacher model).

4. Experimental Setup

Model and Dataset Construction. Following previous works (Yan et al., 2025; Liu et al.; Zeng et al., 2025), we adopt Qwen2.5-Math-7B (Yang et al., 2024) as our default base model. We adopt Qwen3-30B-A3B (Team, 2025) as the teacher model, aligning with the Cross-Family setting described in Section 2.3. We utilize OpenR1-Math-46k-8192 (Yan et al., 2025), a subset of OpenR1-Math-220k (Hugging Face, 2025), as the source for our training data. To facilitate a direct comparison with the off-policy and mixed-policy methods, we sample teacher responses for OpenR1-Math-46k-8192; after filtering incorrect responses via Math-Verify⁵, we obtain a curated set of 35k prompts and corresponding off-policy reasoning traces⁶. Additionally, we conduct experiments using Qwen2.5-Math-1.5B as the student model to evaluate performance under a significantly larger teacher-student capability gap (See Appendix B.3 for more details).

Benchmarks and Metrics. We assess performance across six widely-adopted mathematical reasoning benchmarks: AIME24, AIME25, AMC (Li et al., 2024), Minerva (Lewkowycz et al., 2022), OlympiadBench (He et al., 2024), and MATH500 (Hendrycks et al., 2021). For evaluation metrics, we report **avg@32** for AIME24, AIME25, and AMC to mitigate variance given their smaller dataset sizes.

⁵<https://github.com/huggingface/Math-Verify>

⁶Note that these traces are exclusive to off-policy and mixed-policy methods; TGPO is on-policy and requires only prompts.

For the remaining benchmarks, we report standard **pass@1**. To assess generalization beyond mathematics, we evaluate our model on three out-of-distribution benchmarks: ARC-c (Clark et al., 2018), GPQA-Diamond (Rein et al., 2024) (denoted as GPQA*), and MMLU-Pro (Wang et al., 2024). During inference, we set the sampling temperature to 0.6. Additionally, we shuffle multiple-choice options to mitigate position bias and prevent potential data contamination.

Baseline Methods. We compare our approach against on-policy baselines but also report on off-policy/mixed-policy approaches for completeness. On-Policy Methods categorize into distillation and RLVR. For distillation, we include OP Distill (Lu & Lab, 2025), using the RKL log-ratio as the advantage, and KDRL (Xu et al., 2025), which augments the RL objective with RKL regularization. Additionally, we benchmark four RLVR variants: (1) SimpleRL-Zero, trained with standard rule-based rewards; (2) Oat-Zero (Liu et al.), utilizing Dr.GRPO for simplified advantage computation and loss normalization; (3) PRIME-Zero (Cui et al., 2025), which derives implicit process rewards from policy rollouts and outcome labels; and (4) GRPO++, which eliminates the explicit KL penalty and adds token-level supervision. Off-policy and mixed-policy strategies include: (1) SFT, fine-tuned on teacher-sampled responses and (2) LUFFY (Yan et al., 2025), a mixed-policy method that integrates teacher-sampled trajectories as auxiliary supervision during RLVR. Please refer to Appendix B.1 for detailed training configurations.

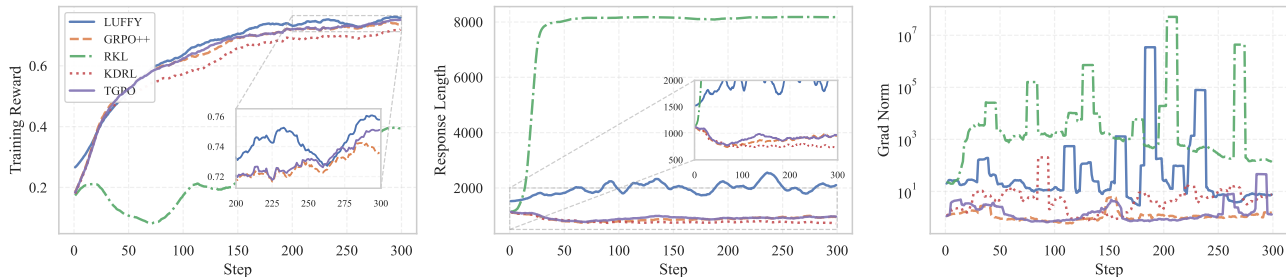


Figure 4. Training Dynamics Analysis. **(Left)** Training reward. TGPO demonstrates robust growth and convergence compared to RKL. **(Middle)** Response length. TGPO avoids RKL’s length explosion and aligns with GRPO++’s stability. **(Right)** Gradient norm. TGPO shows stable optimization compared to the high variance in RKL, KDRL and LUFFY.

5. Experimental Results

5.1. Main Results

Overall Performance. Table 1 reports the performance on in-distribution (ID) math tasks and out-of-distribution (OOD) reasoning benchmarks. TGPO-annealing achieves the best overall performance among all compared 7B-scale methods. Crucially, TGPO demonstrates a significant advantage over other on-policy distillation approaches. It surpasses KDRL by a large margin (45.6 vs. 41.7) and avoids the training collapse observed in OP Distill, proving its superior stability and efficiency. Furthermore, TGPO-annealing outperforms strong baselines from other categories, including the mixed-policy method LUFFY (44.4) and the RLVR method GRPO++ (43.4). Regarding generalization, results highlight the inherent advantage of on-policy distillation for OOD tasks. TGPO-annealing maximizes this benefit, achieving the highest OOD average of 56.8. It not only outperforms SFT (46.1) but also surpasses LUFFY on challenging benchmarks like ARC-c (82.8 vs. 80.1), confirming that our approach effectively enhances complex reasoning while maintaining robust general intelligence.

Regularization vs. Reward Shaping. We further investigate the optimal strategy for incorporating teacher guidance by comparing two TGPO variants: TGPO, which employs guidance as a differentiable policy regularization term, and TGPO_R, which incorporates teacher signals via reward shaping. As shown in the bottom rows of Table 1, TGPO consistently outperforms TGPO_R across both domains (ID: 44.1 vs. 43.6; OOD: 56.0 vs. 53.8). This comparison suggests that enforcing the teacher’s distribution as a regularization term is more effective than implicitly guiding the policy via reward shaping. While reward shaping only modifies the scalar feedback, regularization imposes a direct constraint on the policy update direction, ensuring that the parameters are optimized more effectively leveraging the teacher’s dense supervision.

5.2. Training Dynamics and Stability Analysis

To provide a deeper understanding of the optimization process, we analyze the training dynamics of TGPO compared to the baselines (GRPO++, KDRL, RKL, and LUFFY) across three metrics: training reward, response length, and gradient norm. Figure 4 highlights the effectiveness of TGPO as an on-policy distillation method compared to RKL-based approaches (RKL and KDRL). While RKL suffers from early reward collapse (Left) and severe length explosion ($> 8,000$ tokens, Middle), TGPO demonstrates robust convergence with stable response lengths, mirroring the trajectory of the strong baseline GRPO++. This contrast underscores that TGPO successfully leverages on-policy exploration with teacher supervision to regulate generation, effectively preventing the policy degeneration observed in RKL-based methods. Finally, regarding LUFFY, although it appears to achieve the highest reward, this metric is inflated by its strategy of fixing a ground-truth sample in every group, which likely contributes to the significant volatility observed in its gradient norm (Right).

5.3. Impact of Guidance Scheduling

To validate the linear decay schedule defined in Section 3.2, we compare our strategy against three baselines with varying initial weights w_{init} and decay rates δ : (1) Constant Weight ($w_{\text{init}} = 2e - 3, \delta = 0$); (2) Aggressive Annealing ($w_{\text{init}} = 2e - 2, \delta = 1e - 4$); (3) Continuous Annealing ($w_{\text{init}} = 2e - 3, \delta \approx 6.7e - 6$, decaying to zero at the final step); and (4) Ours ($w_{\text{init}} = 2e - 3, \delta = 1e - 5$, decaying to zero at step 200).

Figure 5 demonstrate that Ours achieves the best overall performance. Aggressive Annealing suffers from significantly suppressed rewards in the early phase, confirming that overly rigid initial constraints hinder the student from exploring diverse reasoning paths. While Constant Weight keeps pace initially, it plateaus prematurely, indicating that permanently enforcing imitation constraints limits the student’s ability to maximize environmental rewards. Most importantly, Ours outperforms Continuous Annealing. al-

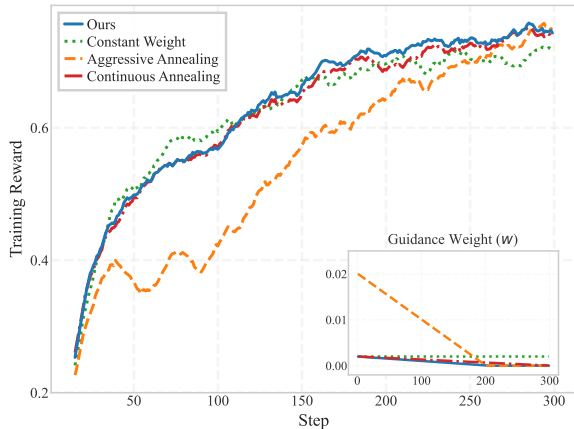


Figure 5. Ablation of annealing schedules. The inset details the guidance weight (w) schedule for each setting. Our method yields the best convergence.

though both strategies start similarly, the performance gap becomes evident in the later stages. This suggests that a transition to a “pure RL phase” (where $w_t = 0$) before the end of training is essential. By removing the imitation constraint at step 200, Ours allows the student to fully detach from the teacher’s distribution and refine its policy solely based on task rewards, thereby attaining the highest final training reward.

5.4. TGPO with Different Teachers

To assess the generalizability of our approach, we investigate the impact of utilizing different teacher models within the TGPO framework. We compare a baseline trained without teacher guidance (No Teacher) against TGPO variants guided by two distinct models: R1-Distill-Qwen-32B and Qwen3-30B-A3B. As shown in Table 2, incorporating teacher guidance generally enhances performance compared to the pure RL baseline. Specifically, utilizing Qwen3-30B-A3B yields the most significant overall improvements, boosting the average accuracy to 58.0%. While R1-Distill-Qwen-32B achieves exceptional performance on GPQA (40.9%), Qwen3-30B-A3B dominates on mathematical benchmarks (AMC, MATH, and Olympiad). This suggests that TGPO effectively capitalizes on the specific strengths of different teachers, demonstrating that our method is model-agnostic and scales effectively with more capable teacher models. We leave the exploration of a broader spectrum of teacher models to future work.

6. Related Work

On-Policy Distillation. MiniLLM (Gu et al., 2023) pioneered on-policy distillation by sampling directly from the student distribution (Eq. 1). This formulation naturally aligns with RL frameworks, such as RLVR. In the context of LLM distillation, Xu et al. (2025) represents the first attempt

Teacher Model	AMC	MATH	Olympiad	GPQA*	Avg.
No Teacher	58.3	82.2	47.3	32.3	55.0
R1-Distill-Qwen-32B	57.8	83.4	47.4	40.9	57.4
Qwen3-30B-A3B	60.2	84.4	49.8	37.4	58.0

Table 2. Ablation study on different teacher models. We compare the performance of TGPO when guided by different teacher policies with a no-teacher baseline.

to combine on-policy distillation with RLVR to train student models. Both these academic works and recent industry implementations (Lu & Lab, 2025) rely on reverse KL (RKL) divergence. However, as we analyze and validate in Section 2, the effectiveness of RKL is heavily contingent on the proximity between the student and teacher distributions. This dependency significantly restricts its applicability in scenarios with severe policy divergence.

Teacher Signal Integration. A critical yet underexplored aspect of distillation is how teacher guidance signals are integrated into the student’s learning process. In this work, we investigate two distinct mechanisms: *reward shaping* and *differentiable regularization*. While previous LLM distillation literature (Xu et al., 2025; Gu et al., 2023; Lu & Lab, 2025) often treats these formulation choices implicitly, we argue that distinguishing between them is crucial for optimization performance. We explicitly compare these approaches and highlight that differentiable regularization offers a more direct learning target from the teacher. We further note that while this distinction has been overlooked in LLM distillation, the challenge of integrating KL regularization is a recognized problem in the broader RL community, with recent studies offering thorough theoretical discussions (Zhang et al., 2025b; Shah et al., 2026).

Discussion over Mixed-Policy. In the context of LLM distillation, mixed-policy approaches (Yan et al., 2025; Zhang et al., 2025a), which leverage samples from the teacher distribution, have achieved competitive results. However, our work remains strictly focused on the on-policy setting. We posit that on-policy learning, by optimizing the student’s generation trajectory, offers greater robustness against distribution mismatch and ensures theoretical consistency with standard RL algorithms. By adhering to a strict on-policy setting, our insights are designed to not only advance LLM distillation but also generalize to fundamental RL research.

7. Conclusion

We present TGPO, an on-policy distillation framework designed to overcome Reverse KL limitations. Compared to the sparse and potentially uninformative signals provided by Reverse KL based algorithms, TGPO incorporates dense and explicit teacher guidance based on the student’s rollout, while maintaining the robustness of on-policy learning. Empirical results across diverse mathematical reasoning

benchmarks demonstrate that TGPO not only outperforms baselines but also exhibits adaptability to various teacher models. Moreover, we demonstrate that applying guidance via differentiable regularization, coupled with a linear decay schedule, is essential for stable convergence and continued self-improvement. We hope our findings provide a theoretically grounded and practically effective direction for future advancements in LLM alignment.

Impact Statement

This work introduces TGPO, a method for enhancing the reasoning capabilities of Large Language Models through efficient on-policy distillation. By enabling smaller student models to achieve high-level performance previously reserved for massive teacher models, our approach contributes to the democratization of AI, reducing the computational resources and environmental costs required for deploying advanced reasoning systems. There are no specific negative societal consequences that we feel must be highlighted beyond those generally associated with the development of more capable language models.

References

- Agarwal, R., Vieillard, N., Zhou, Y., Stanczyk, P., Garea, S. R., Geist, M., and Bachem, O. On-policy distillation of language models: Learning from self-generated mistakes. In *The twelfth international conference on learning representations*, 2024.
- Chen, H., Tu, H., Wang, F., Liu, H., Tang, X., Du, X., Zhou, Y., and Xie, C. Sft or rl? an early investigation into training rl-like reasoning large vision-language models. *arXiv preprint arXiv:2504.11468*, 2025.
- Chu, T., Zhai, Y., Yang, J., Tong, S., Xie, S., Schuurmans, D., Le, Q. V., Levine, S., and Ma, Y. Sft memorizes, rl generalizes: A comparative study of foundation model post-training. *arXiv preprint arXiv:2501.17161*, 2025.
- Clark, P., Cowhey, I., Etzioni, O., Khot, T., Sabharwal, A., Schoenick, C., and Tafjord, O. Think you have solved question answering? try arc, the ai2 reasoning challenge. *arXiv preprint arXiv:1803.05457*, 2018.
- Cui, G., Yuan, L., Wang, Z., Wang, H., Zhang, Y., Chen, J., Li, W., He, B., Fan, Y., Yu, T., et al. Process reinforcement through implicit rewards. *arXiv preprint arXiv:2502.01456*, 2025.
- Gu, Y., Dong, L., Wei, F., and Huang, M. Minillm: Knowledge distillation of large language models. *arXiv preprint arXiv:2306.08543*, 2023.
- Guo, D., Yang, D., Zhang, H., Song, J., Zhang, R., Xu, R., Zhu, Q., Ma, S., Wang, P., Bi, X., et al. Deepseek-rl: Incentivizing reasoning capability in llms via reinforcement learning. *arXiv preprint arXiv:2501.12948*, 2025.
- He, C., Luo, R., Bai, Y., Hu, S., Thai, Z., Shen, J., Hu, J., Han, X., Huang, Y., Zhang, Y., et al. Olympiadbench: A challenging benchmark for promoting agi with olympiad-level bilingual multimodal scientific problems. In *Proceedings of the 62nd Annual Meeting of the Association for Computational Linguistics (Volume 1: Long Papers)*, pp. 3828–3850, 2024.
- He, J., Liu, J., Liu, C. Y., Yan, R., Wang, C., Cheng, P., Zhang, X., Zhang, F., Xu, J., Shen, W., et al. Skywork open reasoner 1 technical report. *arXiv preprint arXiv:2505.22312*, 2025.
- Hendrycks, D., Burns, C., Kadavath, S., Arora, A., Basart, S., Tang, E., Song, D., and Steinhardt, J. Measuring mathematical problem solving with the math dataset. *arXiv preprint arXiv:2103.03874*, 2021.
- Hinton, G., Vinyals, O., and Dean, J. Distilling the knowledge in a neural network. *arXiv preprint arXiv:1503.02531*, 2015.
- Hugging Face. Open rl: A fully open reproduction of deepseek-rl, January 2025. URL <https://github.com/huggingface/open-rl>.
- Jaech, A., Kalai, A., Lerer, A., Richardson, A., El-Kishky, A., Low, A., Helyar, A., Madry, A., Beutel, A., Carney, A., et al. Openai o1 system card. *arXiv preprint arXiv:2412.16720*, 2024.
- Lewkowycz, A., Andreassen, A., Dohan, D., Dyer, E., Michalewski, H., Ramasesh, V., Slone, A., Anil, C., Schlag, I., Gutman-Solo, T., et al. Solving quantitative reasoning problems with language models, 2022. URL <https://arxiv.org/abs/2206.14858>, 1, 2022.
- Li, J., Beeching, E., Tunstall, L., Lipkin, B., Soletskyi, R., Huang, S., Rasul, K., Yu, L., Jiang, A. Q., Shen, Z., et al. NuminaMath: The largest public dataset in ai4maths with 860k pairs of competition math problems and solutions. *Hugging Face repository*, 13(9):9, 2024.
- Liu, Z., Chen, C., Li, W., Qi, P., Pang, T., Du, C., Lee, W. S., and Lin, M. Understanding rl-zero-like training: A critical perspective, 2025. URL <https://arxiv.org/abs/2503.20783>.
- Lu, K. and Lab, T. M. On-policy distillation. *Thinking Machines Lab: Connectionism*, 2025. doi: 10.64434/tml.20251026. <https://thinkingmachines.ai/blog/on-policy-distillation>.
- Rein, D., Hou, B. L., Stickland, A. C., Petty, J., Pang, R. Y., Dirani, J., Michael, J., and Bowman, S. R. Gpqa: A

- graduate-level google-proof q&a benchmark. In *First Conference on Language Modeling*, 2024.
- Shah, V., Obando-Ceron, J., Jain, V., Bartoldson, B., Kailkhura, B., Mittal, S., Berseth, G., Castro, P. S., Bengio, Y., Malkin, N., Jain, M., Venkatraman, S., and Courville, A. A comedy of estimators: On kl regularization in rl training of llms, 2026. URL <https://arxiv.org/abs/2512.21852>.
- Shao, Z., Wang, P., Zhu, Q., Xu, R., Song, J., Bi, X., Zhang, H., Zhang, M., Li, Y., Wu, Y., et al. Deepseekmath: Pushing the limits of mathematical reasoning in open language models. *arXiv preprint arXiv:2402.03300*, 2024.
- Team, G., Riviere, M., Pathak, S., Sessa, P. G., Hardin, C., Bhupatiraju, S., Hussenot, L., Mesnard, T., Shahriari, B., Ramé, A., et al. Gemma 2: Improving open language models at a practical size. *arXiv preprint arXiv:2408.00118*, 2024.
- Team, K., Du, A., Gao, B., Xing, B., Jiang, C., Chen, C., Li, C., Xiao, C., Du, C., Liao, C., et al. Kimi k1. 5: Scaling reinforcement learning with llms. *arXiv preprint arXiv:2501.12599*, 2025.
- Team, Q. Qwen3 technical report, 2025. URL <https://arxiv.org/abs/2505.09388>.
- Wang, Y., Ma, X., Zhang, G., Ni, Y., Chandra, A., Guo, S., Ren, W., Arulraj, A., He, X., Jiang, Z., et al. Mmlu-pro: A more robust and challenging multi-task language understanding benchmark. *Advances in Neural Information Processing Systems*, 37:95266–95290, 2024.
- Xu, H., Zhu, Q., Deng, H., Li, J., Hou, L., Wang, Y., Shang, L., Xu, R., and Mi, F. Kdrl: Post-training reasoning llms via unified knowledge distillation and reinforcement learning. *arXiv preprint arXiv:2506.02208*, 2025.
- Yan, J., Li, Y., Hu, Z., Wang, Z., Cui, G., Qu, X., Cheng, Y., and Zhang, Y. Learning to reason under off-policy guidance, 2025. URL <https://arxiv.org/abs/2504.14945>, 2025.
- Yang, A., Zhang, B., Hui, B., Gao, B., Yu, B., Li, C., Liu, D., Tu, J., Zhou, J., Lin, J., Lu, K., Xue, M., Lin, R., Liu, T., Ren, X., and Zhang, Z. Qwen2.5-math technical report: Toward mathematical expert model via self-improvement. *arXiv preprint arXiv:2409.12122*, 2024.
- Yu, Q., Zhang, Z., Zhu, R., Yuan, Y., Zuo, X., Yue, Y., Fan, T., Liu, G., Liu, L., Liu, X., et al. Dapo: An open-source llm reinforcement learning system at scale, 2025. URL <https://arxiv.org/abs/2503.14476>, 2025.
- Zeng, W., Huang, Y., Liu, W., He, K., Liu, Q., Ma, Z., and He, J. 7b model and 8k examples: Emerging reasoning with reinforcement learning is both effective and efficient. <https://hkust-nlp.notion.site/simplerl-reason>, 2025. Notion Blog.
- Zhang, W., Xie, Y., Sun, Y., Chen, Y., Wang, G., Li, Y., Ding, B., and Zhou, J. On-policy rl meets off-policy experts: Harmonizing supervised fine-tuning and reinforcement learning via dynamic weighting, 2025a. URL <https://arxiv.org/abs/2508.11408>.
- Zhang, Y., Liu, Y., Yuan, H., Yuan, Y., Gu, Q., and Yao, A. C.-C. On the design of kl-regularized policy gradient algorithms for llm reasoning, 2025b. URL <https://arxiv.org/abs/2505.17508>.

A. Theoretical Analysis of RKL Instability

In this appendix, we provide the formal derivations referenced in Section 2.2. We analyze the gradient dynamics of the Reverse KL (RKL) objective to demonstrate why it suffers from high variance and instability, particularly when the student policy π_θ deviates from the teacher policy π_T (the **Rejection** regime).

A.1. Gradient Derivation of the RKL Objective

Recall the RKL objective defined in Eq. 1:

$$\begin{aligned} \mathcal{J}_{\text{RKL}}(\theta) &= \mathbb{E}_{x \sim \mathcal{D}} D_{\text{KL}}(\pi_\theta \| \pi_T) \\ &= \mathbb{E}_{x \sim \mathcal{D}, y \sim \pi_\theta(\cdot|x)} \left[\log \frac{\pi_\theta(y|x)}{\pi_T(y|x)} \right]. \end{aligned} \quad (7)$$

For a fixed prompt x , let $J(\theta) = D_{\text{KL}}(\pi_\theta \| \pi_T)$. Using the log-derivative trick (REINFORCE estimator), the gradient with respect to θ is:

$$\begin{aligned} \nabla_\theta J(\theta) &= \nabla_\theta \mathbb{E}_{y \sim \pi_\theta} [\log \pi_\theta(y|x) - \log \pi_T(y|x)] \\ &= \mathbb{E}_{y \sim \pi_\theta} \left[\nabla_\theta \log \pi_\theta(y|x) \cdot \left(\log \frac{\pi_\theta(y|x)}{\pi_T(y|x)} \right) + \nabla_\theta \left(\log \frac{\pi_\theta(y|x)}{\pi_T(y|x)} \right) \right] \\ &= \mathbb{E}_{y \sim \pi_\theta} [\nabla_\theta \log \pi_\theta(y|x) \cdot (\log \rho(y) + 1)], \end{aligned} \quad (8)$$

where $\rho(y) = \frac{\pi_\theta(y|x)}{\pi_T(y|x)}$ is the density ratio. Note that the term resulting from $\mathbb{E}[\nabla_\theta \log \pi_\theta] = 0$ is often omitted, but strictly speaking, the gradient is weighted by the term $(\log \rho(y) + 1)$. In the context of RL with intrinsic rewards (as discussed in Section 2.2), the RKL term acts as a negative reward. The effective gradient update applied to the student is proportional to:

$$g(y) \propto -\nabla_\theta \log \pi_\theta(y|x) \cdot \log \rho(y). \quad (9)$$

A.2. Instability in the Rejection Regime

We now analyze the behavior of this gradient. Note that while language models generate tokens autoregressively (i.e., $\pi(y|x) = \prod_{t=1}^L \pi(y_t|y_{<t}, x)$), our analysis focuses on the complete trajectory level y . This perspective is crucial because the density ratio accumulates over the sequence length, amplifying the variance.

Unbounded Gradient Magnitude. Consider a ‘‘bad’’ sample y_{bad} in the Rejection regime which defined as $\rho(y) \gg 1$, i.e., $\pi_\theta(y|x) \gg \pi_T(y|x)$. This occurs when the student policy assigns a non-negligible probability to a sample that the teacher rejects. Formally, assume $\pi_\theta(y_{\text{bad}}|x) \geq \delta$ for some constant $\delta > 0$, while $\pi_T(y_{\text{bad}}|x) \leq \epsilon$ with $\epsilon \rightarrow 0$.

The log-density ratio is then bounded below by:

$$\log \rho(y_{\text{bad}}) = \log \pi_\theta(y_{\text{bad}}|x) - \log \pi_T(y_{\text{bad}}|x) \geq \log \delta - \log \epsilon = \log \left(\frac{\delta}{\epsilon} \right). \quad (10)$$

As $\epsilon \rightarrow 0$, the term $\log(\delta/\epsilon) \rightarrow \infty$. Consequently, the gradient scaling factor $|\log \rho(y_{\text{bad}})|$ becomes unbounded, leading to extreme variance in the gradient estimator. This instability is particularly acute in cross-family distillation, where structural and reasoning pattern discrepancies frequently cause the teacher to assign negligible probability to valid student trajectories. This theoretical analysis directly explains the sharp gradient spikes observed in Figure 2 (Middle).

Variance Explosion. The stability of the stochastic gradient descent is governed by the variance of the gradient estimator. Since $\text{Var}(X) = \mathbb{E}[X^2] - (\mathbb{E}[X])^2$, the variance is dominated by the second moment of the gradient norm. We approximate the behavior in the Rejection regime by analyzing this second moment:

$$\mathbb{E}_{y \sim \pi_\theta} [|\nabla_\theta \log \pi_\theta(y|x)|^2 \cdot (\log \rho(y))^2]. \quad (11)$$

As $\pi_T(y|x) \rightarrow 0$, the squared log-ratio term $(\log \rho(y))^2$ grows quadratically with the magnitude of the divergence. This causes the second moment (and consequently the variance) to explode. Such extreme variance destabilizes momentum-based optimizers like Adam, potentially leading to catastrophic forgetting or the destruction of previously learned features.

A.3. Asymmetry of Reward Scaling

In Section 2.2, we argued that RKL imposes an asymmetric optimization landscape. We formalize this by analyzing the intrinsic reward $r_{\text{int}}(y) = -\log \rho(y) = \log \frac{\pi_T(y|x)}{\pi_\theta(y|x)}$.

- **Positive Rewards are Probabilistically Suppressed (Consensus Regime):** High positive rewards occur when the teacher implies the sample is much better than the student estimates, i.e., $\pi_T(y|x) \gg \pi_\theta(y|x)$. However, since trajectories are sampled from the student π_θ , the probability of observing such events is fundamentally limited by π_θ itself. As $\pi_\theta(y|x) \rightarrow 0$ (necessary for a large reward), the sampling probability vanishes. Thus, the student effectively never experiences large positive reinforcement, restricting the effective reward magnitude in practice.
- **Negative Penalties are Unbounded (Rejection Regime):** Conversely, large penalties occur when $\pi_\theta(y|x) \gg \pi_T(y|x)$. By definition, this condition implies that π_θ is high, meaning the student is *highly likely* to sample these trajectories. Consequently, the estimator is frequently exposed to these unbounded penalty terms ($-\log \rho(y) \gg 0$). This asymmetry—where the gradient is dominated by frequent, large negative updates rather than positive ones—also drives the variance explosion and instability.

Impact on Batch Dynamics. Consider a batch $\mathcal{B} = \{y_1, \dots, y_B\}$. The total gradient is the average of individual sample gradients. Suppose $(B - 1)$ samples are in the Consensus regime (bounded rewards), while a single outlier sample y_k falls into the Rejection regime where $\pi_T(y_k|x) \rightarrow 0$.

Since the log-ratio $|\log \rho(y_k)| \gg |\log \rho(y_i)|$ for $i \neq k$, the gradient contribution of y_k overwhelms the signal from the rest of the batch:

$$\nabla_\theta J \approx \frac{1}{B} \left(\underbrace{\nabla_\theta \log \pi_\theta(y_k) \cdot \log \rho(y_k)}_{\text{Dominant Term}} + \underbrace{\sum_{i \neq k} \nabla_\theta \log \pi_\theta(y_i) \cdot \log \rho(y_i)}_{\text{Negligible Relative Contribution}} \right). \quad (12)$$

This implies that the optimization landscape in RKL is effectively *penalty-driven*: the update direction is primarily determined by the urgent need to suppress the probability of the single “bad” sample y_k , rather than reinforcing the majority of “good” samples. This mechanism directly leads to the high-variance updates and “catastrophic instability” described in the main text.

A.4. Lack of Directional Guidance

Finally, we contrast the optimization mechanics of the RKL gradient with Forward KL (FKL) or Supervised Fine-Tuning (SFT).

- **SFT/FKL (Target-driven):** The gradient is approximated as $\nabla J_{\text{SFT}} \approx -\nabla_\theta \log \pi_\theta(y^*)$, where y^* is a sample from the teacher (or ground truth). This gradient explicitly *pulls* the student’s probability mass towards the specific target token y^* . It provides a clear, constructive signal: “Increase the probability of this specific token.”
- **RKL (Avoidance-driven):** In the Rejection regime, the gradient update is proportional to $-\nabla_\theta \log \pi_\theta(y) \cdot \log \rho(y)$, where $\log \rho(y) \gg 0$. Since we perform gradient descent, this update explicitly *pushes* the student’s probability mass away from the sampled token y . The signal is purely destructive: “Decrease the probability of this specific token.”

The High-Dimensionality Problem. Mathematically, minimizing the probability of a specific token y ($\pi_\theta(y) \downarrow$) necessitates increasing the probability of the complement set ($\sum_{y' \neq y} \pi_\theta(y') \uparrow$) to maintain normalization. However, the RKL gradient is **agnostic regarding which y' should receive this redistributed mass.**

In the context of LLMs with a vocabulary size $|V|$ (often $> 32,000$), reducing the probability of one “bad” token provides negligible information about the location of the “good” tokens. The optimizer effectively has to eliminate incorrect tokens one by one. Without the explicit guidance provided by SFT, the student must rely on inefficient random exploration to discover the high-probability regions of the teacher, exacerbating the instability and slow convergence.

B. Experimental Details

In this appendix, we provide detailed experimental settings, hyperparameter configurations, and additional empirical results.

B.1. Detailed Setup

Training Dataset. In this work, all experiments utilize a unified dataset derived from a subset of OpenR1-Math-46k-8192. We retained the original prompts from NuminaMath 1.5 but reconstructed the reasoning traces to facilitate a controlled comparison across different paradigms. Specifically, although our proposed TGPO is an on-policy method that requires only prompts (generating its own rollouts during training), we explicitly constructed a static set of off-policy traces to train the off-policy and mixed-policy baselines. To this end, we employed Qwen3-30B-A3B as the teacher model to re-sample reasoning trajectories, which were subsequently validated using Math-verify. The final curated dataset consists of approximately 35,000 prompts, paired with valid teacher-generated traces to support the baseline implementations.

Training Configuration. In addition to Qwen2.5-Math-7B, we extend our evaluation to the smaller Qwen2.5-Math-1.5B. For main experiments, we utilize the significantly larger Qwen3-30B-A3B as the teacher model. This setup deliberately creates a substantial capability gap between the teacher and the student, simulating the **Rejection** regime described in our analysis. For the in-family experiments discussed in Section 2.3, we substitute the teacher model with Qwen2.5-Math-7B while keeping all other experimental configurations identical. To ensure a fair comparison, we maintain a fixed sampling budget of $K = 8$ per prompt for all RL-trained models. The learning rate is kept constant at 1×10^{-6} . All experiments are conducted on a cluster of 8 NVIDIA A100 GPUs. The training duration is set to 300 steps for RL models and 3 epochs for SFT baselines. Our implementation is built upon the verl framework⁷, utilizing vLLM⁸ for efficient rollout generation.

Model Configuration. The native context window of Qwen2.5-Math-7B and Qwen2.5-Math-1.5B (4,096 tokens) is insufficient for processing the lengthy reasoning traces present in off-policy samples. To address this, we modified the model configuration by scaling the RoPE base frequency (θ) from 10,000 to 40,000 and extending the context window size to 16,384 tokens. Conversely, Qwen3-30B-A3B inherently supports a sufficiently large context window; thus, its RoPE configuration remains unchanged. Furthermore, to ensure consistency between the student and teacher models, we resized the vocabulary dimensions of both models to a unified size.

SFT Implementation. For all SFT baselines, we utilize the same dataset comprising Qwen3-30B-A3B generated prompts and reasoning traces as used in our proposed method. We adhere to the training protocols established by OpenR1 (Hugging Face, 2025), which have been verified to reproduce the performance of DeepSeek-R1’s distilled models. Specifically, we train each model for 3 epochs with a global batch size of 64 and a learning rate of 5×10^{-5} . We employ a learning rate warmup ratio of 0.1 and set the maximum sequence length to 16,384.

B.2. System Prompt

Your task is to follow a systematic, thorough reasoning process before providing the final solution. This involves analyzing, summarizing, exploring, reassessing, and refining your thought process through multiple iterations. Structure your response into two sections: Thought and Solution. In the Thought section, present your reasoning using the format: “<think>\n thoughts </think>\n”. Each thought should include detailed analysis, brainstorming, verification, and refinement of ideas. After “</think>\n” in the Solution section, provide the final, logical, and accurate answer, clearly derived from the exploration in the Thought section. If applicable, include the answer in `\boxed{}` for closed-form results like multiple choices or mathematical solutions.

User: {QUESTION}

Assistant: <think>

⁷<https://github.com/verl-project/verl>

⁸<https://github.com/vllm-project/vllm>

Model	AIME 24	AIME 25	AMC	MATH-500	Minerva	Olympiad	Avg.
Qwen2.5-Math-1.5B	7.2	3.6	26.4	28.0	9.6	21.2	16.0
LUFFY	5.8	4.9	32.6	64.0	22.4	24.7	25.7
GRPO++	10.1	7.4	41.8	69.4	28.3	35.9	32.2
KDRL	0.9	0.3	5.9	11.4	5.1	4.7	4.7
OP Distill	1.7	0.4	18.8	45.2	16.2	14.7	16.2
TGPO_R	11.6	8.2	43.3	71.2	26.8	35.1	32.7
TGPO-annealing	11.8	7.8	43.0	71.4	30.5	36.6	33.5

Table 3. Performance evaluation based on Qwen2.5-Math-1.5B. The teacher model employed is Qwen3-30B-A3B. All models are evaluated under a unified setting. Bold indicates the best result.

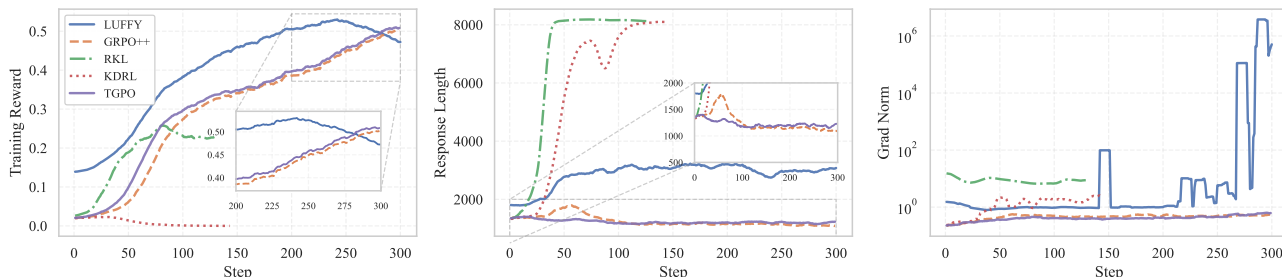


Figure 6. Training Dynamics Analysis. **(Left)** Training reward. TGPO demonstrates robust growth and convergence compared to RKL and KDRL. **(Middle)** Response length. TGPO avoids RKL’s length explosion and aligns with GRPO++’s stability. **(Right)** Gradient norm. TGPO shows stable optimization compared to the high variance in RKL, KDRL and LUFFY.

B.3. Analysis of Experiments on the 1.5B Model

B.3.1. OVERALL PERFORMANCE

To further validate the scalability and robustness of our proposed method, we conducted experiments using Qwen2.5-Math-1.5B as the student and Qwen3-30B-A3B as the teacher. This setup evaluates the performance of various paradigms under a significant capability gap. Our experiments include GRPO++, RKL, KDRL, LUFFY, and our proposed TGPO_R and TGPO-annealing. The experimental results on the Qwen2.5-Math-1.5B student model, as summarized in Table 3, provide several key insights into the behavior of different RL paradigms under a large teacher-student capability gap:

Superiority of TGPO Variants. Our proposed TGPO methods consistently outperform all on-policy and off-policy baselines across nearly all benchmarks. Notably, TGPO-annealing achieves the highest average score of 33.5%. This improvement demonstrates that by effectively leveraging teacher-guided signals without being constrained by rigid KL divergence penalties, TGPO allows smaller student models to explore and internalize complex reasoning patterns more efficiently.

Failure of RKL-based Distillation. A critical observation is the near-total failure of KDRL (4.7% Avg.), which relies on Reverse KL (RKL) divergence. In this “Rejection” regime where the teacher is significantly more advanced than the student, the student struggles to produce samples that align with the high-precision distribution of the teacher. RKL-based methods tend to collapse or penalize the student excessively for its inability to mimic the teacher’s exact traces, leading to a “stability trap” where the model fails to learn meaningful reasoning capabilities. Due to the rapid collapse of training curves for KDRL and RKL, we terminated their training once the generation length reached the maximum context window. For a fair and robust assessment, we report the performance based on their best-performing checkpoints.

Comparison with Other Baselines. While GRPO++ shows competitive results (32.2% Avg.), it still falls short of the TGPO variants. This suggests that while standard on-policy RL can elicit reasoning, the additional guidance provided by the teacher’s relative scoring in TGPO provides a more robust gradient signal, especially for smaller models that require more directed exploration. Moreover, LUFFY shows lower performance in this specific 1.5B setup compared to 7B, suggesting that off-policy traces alone may not be sufficient for very small models to bridge the capability gap without the dynamic feedback loop provided by TGPO.

B.3.2. TRAINING DYNAMIC

To gain a deeper understanding of the observed performance gaps, we analyze the training dynamics of the 1.5B student model across various RL paradigms. Figure 6 illustrates the evolution of training reward, response length, and gradient norm during the first 300 steps of optimization.

Robust Growth in Training Reward. As shown in the left panel of Figure 6, TGPO exhibits a robust and stable growth in training reward, consistently converging to higher values compared to RKL-based methods. In contrast, KDRL fails to show any meaningful improvement in reward from the onset of training, which directly correlates with its near-total failure in final benchmark performance.

Effective Mitigation of Length Explosion. The middle panel reveals a critical failure mode in RKL-based distillation. Both RKL and KDRL suffer from an immediate “length explosion,” where the student’s response length rapidly saturates at the maximum context window of 8,192 tokens. Conversely, TGPO avoids this explosion, maintaining a stable and efficient response length that aligns closely with GRPO++, suggesting a healthier exploration of the reasoning space.

Gradient Stability under Capability Gaps. The right panel highlights the optimization stability of each method. TGPO maintains a remarkably stable and low gradient norm throughout the training process. This contrasts sharply with the high variance observed in RKL and KDRL, as well as the significant gradient spikes exhibited by LUFFY. This stability underscores that TGPO provides a more reliable and directed gradient signal, which is essential for eliciting reasoning capabilities in small-scale models when the teacher-student capability gap is vast.

These dynamics confirm that TGPO effectively navigates the Rejection regime by integrating the teacher guidance.